Scientia Iranica C (2016) 23(3), 1117–1127

Sharif University of Technology
Scientia Iranica
Transactions C: Chemistry and Chemical Engineering
www.scientiairanica.com

Ionic Polymer-Metal Composites (IPMC) from recycled Flemion® membrane used in chlor-alkali industry

S. Taghavi, F. Mohammadi* and J. Barzin

Iran Polymer and Petrochemical Institute, Tehran, P.O. Box 14965/115, Iran.

Received 10 November 2014; received in revised form 25 July 2015; accepted 19 October 2015

KEYWORDS
Recycle-based Flemion®;
Ionic polymer metal composite;
Bending motion;
Actuator.

Abstract. A cost effective IPMC was fabricated by using recycled Flemion® membrane from chlor-alkali industry. An even distribution of platinum particles on the surface and the bulk was shown by line SEM-EDX. Pt particles and the stiffness of the recycled IPMC were gradually increasing during impregnation-reduction process to form a conventional fractured metallic surface layer displaying discrete islands according to SEM photographs. A highly reproducible current-time diagram was obtained at even low voltage despite the fact that there was no observable motion and offset current due to water electrolysis by chronoamperometry. However, the sensible motion was observed after 1.5 V with a significant increase in current and appearance of offset current developing with voltage. Due to capacitive characteristics of the recycled IPMC, peak current decreased with frequency, linearly, while the plateau current was observed only at low frequencies or time periods ($T_p > 5\tau$). The normalized maximum tip force generated at different voltages along with tip displacement and Young's modulus were measured by load cell and compared with those of a Nafion®-based IPMC (N-IPMC). Very close values were obtained confirming that recycling did not have a sensible effect on the mechanics of the recycled IPMC.

1. Introduction

Electroactive polymers (EAP) are a member of polymer family, which can exhibit a large deflection due to the electrical stimuli. Ionic Polymer Metal Composites (IPMC) are classified into EAPs, which are constructed of one thin ion exchange membrane as matrix and two metallic thin films on both sides as electrodes. The IPMC polymer matrix is made of a hydrophobic polymer backbone and hydrophilic anionic side chains and forms clusters of concentrated anions which neutralize cations and water within the polymer network. When the IPMC is hydrated, the positive ions (such as lithium or sodium ions) can move freely inside the membrane, which is attributed to the immobilization of negative ions due to bond with carbon chain of polymer. Exerting an electric field with a relatively low activation voltage (1-5 V) forces the hydrated cations to move to cathode side while the anions are still fixed in place. This procedure, accompanied by transportation of solvent molecules and the associated interactions, leads to bending motion in an IPMC. Deforming capability of IPMC introduces this group of polymeric materials with a great potential as soft robotic actuator, artificial muscles, and dynamic sensors in a broad size range from micro-to-macro scale [1-3]. One of the concerning problems in working with IPMCs is high cost, which is fairly incommodious. The most contributing factors in the IPMC's cost include: polymer, electrode, and the fabrication method. The polymer material generally used as membrane in IPMCs is commonly made of expensive perfluorinated ionomers, such as commercially available Nafion®, Flemion®, or Aciplex® membranes; on the other side,

*. *Corresponding author. Tel.: +98 21 48662455; Fax: +98 21 44580032*
E-mail address: f.mohammadi@ippi.ac.ir (F. Mohammadi)

gold or platinum are usually considered as electrode materials which cause further increase in the final manufacturing cost of IPMCs.

It is necessary to note that Flemion® is a perfluorinated carboxylic acid membrane developed by Asahi Glass, Japan, while Nafion® and Aciplex® are perfluorinated sulfonic acid membranes developed by Du pont, USA, and Asahi Kasei, Japan, respectively. This creates some fundamental mechanical response differences between them. Flemion® shows improved performance as actuator material compared to Nafion®, basically due to a higher ion exchange capacity and better mechanical strength so that it will deform with no back relaxation under applied electrical stimulus, i.e. deformation is stable or even increases as long as the voltage is applied quasi-statically [4]. That is why Felemion membrane was selected for consideration in this study.

Furthermore, there are several methods for fabrication of IPMC's, including electroless plating, sputtering, taping with conductive films, and so on. Among them, electroless plating is the most common fabrication method employed so far, which is not only time consuming, but also a costly process due to utilization of special precious metal complex salts [5]. Shahinpoor and Kim proposed a new method by which the physical loading of silver and palladium particles as conductive phase in IPMC is considered [6]. Fang et al. used a combination of nickel and gold particles in manufacturing procedure of IPMC [7]. Moreover, lots of other investigations have sought new ways in order to reduce the economic issues of IPMC, which show the attempt to make this class of EAP family more affordable despite their unique characteristics. An electro-active polymer, which can be used as sensor and actuator, was developed by Wang et al. based on the sulfonated poly (styrene-b-ethylene-co-butylene-b-styrene) ionic membrane through electroless plating. It has also been reported that the commercially available product of SSEBS is less expensive than Nafion® [8]. Luqman et al. also reported the actuation performance of cost-effective sulfonated polystyrene (s-PS)-based IPMC and compared it with that of a Nafion®-based IPMC (N-IPMC). They claimed that an economically feasible sulfonated PS could be applied for IPMC application [9]. There are several models available to describe bending motion of an IPMC. These models are generally based on an equivalent circuit representation that is related to the electrical, mechanical, and electromechanical properties of the material. Also, more lumped models are available by which input parameters, such as voltage or current, are converted to the output parameters – tip displacement, force, etc. [10-12]. There are a few available finite element models for an IPMC; for example, Jung and Toi developed a finite element model which can be used as a computational tool for the evaluation and design of Flemion®-based IPMC [13].

Unlike previous studies, which either focused on metallic approaches to reduce the final cost of IPMC or switched to other types of ionomers as membrane material, we, here, introduce a novel and affordable method which can be easily used in industrial scale based on recycling the used membranes of some other related industries. Perfluorinated membranes are widely used in different industries, e.g. Chlor-Alkali (CA) and water electrolysis, fuel cells, and so on, which are considered unusable after their service life. These industrial wastages are quaintly a very rich source for manufacturing the membrane used in IPMCs. We have extensively investigated recycling of Nafion® and Flemion® composite membranes from CA industry [14,15]. Here, a new method of IPMC manufacturing is reported, in which the Flemion® as the polymer material is recycled from composite membranes used in CA industry. The recycling of used Nafion® membrane from a PEM fuel cell was also reported earlier [16]. The results obtained by several tests performed in our laboratory on the recycled CA membranes show almost similar conductivity, ion exchange capacity, morphology, and mechanical properties to those of a neat membrane. The morphology, electrical, mechanical performance, and deformation of the IPMC, having recycled Flemion®-based membrane (RF-IPMC), were thus investigated using SEM, SEM-EDX, chronoamperometry, load cell measurement, image processing, respectively, and then compared with those of a new (N-IPMC).

2. Experimental method

2.1. Martials

Tetraammineplatinum (II) chloride hydrate, $[Pt(NH_3)_4]Cl_2 \times H_2O$, was purchased from Alfa-Acer. Sodium borohydride, lithium chloride, hydrochloric acid, and ammonium hydroxide were obtained from Merck Co. Recycled Flemion®-based membrane was obtained from used membrane out of a local CA plant.

2.2. RF-IPMC fabrication

Recycled perfluorosulfonated membrane was cut into 1 cm×3 cm×165 μm rectangular samples for electroless plating via impregnation-reduction process, which is proposed by Shahinpoor and Kim [5]. This process is accomplished in four steps:

1. Surface treatment of recycled membrane (roughening);
2. Adsorption (ion exchange);
3. Reduction (primary plating);
4. Developing (secondary plating);

which are simply explained here:

1. Surface treatments (roughening): At this step, using abrasive paper (180 mesh), surface roughness of the membrane was increased in order to enhance electroless plating and to access the highest possible interfacial area between the polymer and metal composite. Then, the membrane film was immersed into deionized (DI) water for 15 minutes and in an ultrasonic cleaner in order to wipe the residue off the surface. Removing the contaminations from the surface and hydrogenating the sulphonated groups in the membrane were performed using 2N HCL solution, which was in boiling state at 90°C for 30 minutes. Finally, the sample was rinsed with DI boiling water in order to wash out the residual acid and to swell the film.

2. Adsorption (ion exchange): Solution of platinum complex (50 mg platinum and 50 ml water) was prepared. Adding 1 ml of 5% ammonium hydroxide solution for neutralization, the membrane sample was immersed into the solution of platinum complex at room temperature for 24 hours. In this process, hydronium ion (H^+), which existed inside the recycled membrane, was exchanged with $[Pt(NH_3)_4]^{2+}$ ion of complex solution.

3. Reduction (primary plating): At this step, the prepared membrane was rinsed by DI water and set into water while being stirred at 40°C, in which 2 ml of 5% sodium borohydride solution was added every 30 minutes. This process was repeated for 7 times in which the temperature gradually increased up to 60°C. Finally, 20 ml of 5% sodium borohydride solution was added to the container in which the recycled membrane was set. During this process, the Pt^{2+} ion reduced as the metallic ion on the surface and metallic cations of Pt complex formed a black colored layer on the two sides of membrane, which was due to the presence of sodium borohydride as the reducing agent.

4. Developing (secondary plating): To increase the thickness of metallic electrode and to decrease the surface resistance, the membrane was rinsed by DI water and then the steps 2 and 3 were repeated for 6 times. The membrane was then washed again and set in a container of 0.1N HCL. In order to enhance the deformation response of IPMC, the sample was finally set in 1.5 N NaCl solution for one week.

2.3. Instrumentation

Scanning Electron Microscopy (SEM) (Tescan VEGA-II) was used to study the morphology, particle distribution, and the thickness of electrodes of IPMC as well as the recycled membrane. Transmitted amplitude through the recycled IPMC is determined as a function of time for a constant voltage by Potentiostat-glvanostat (PGSTAT 30 Autolab) apparatus via Chronoamperometry method. The tip blocking force generated by IPMCs was measured by load cell WZA1203-N. In order to quantify the deflection capabilities of the recycled IPMC, an observation test was performed by a digital camera and image processing software. Photos taken from deflected sample in different time intervals show the amount of deviation angle in comparison to the initial state.

3. Results and discussions

3.1. SEM morphology and EDX

Figure 1(a) and (b) illustrate the cross-section view of the recycled membrane covered by platinum electrodes on both sides. Figure 1(a) shows metallic electrode as a thin layer with thickness of 10 μm after double plating, while Figure 1(b) illustrates metallic electrode of 18 μm thickness after five-time depositing process. Based on these pictures, it appears that platinum particles gradually grow on the primary layers due to impregnation-reduction process. The slow distribution of platinum particles inside the recycled membrane may

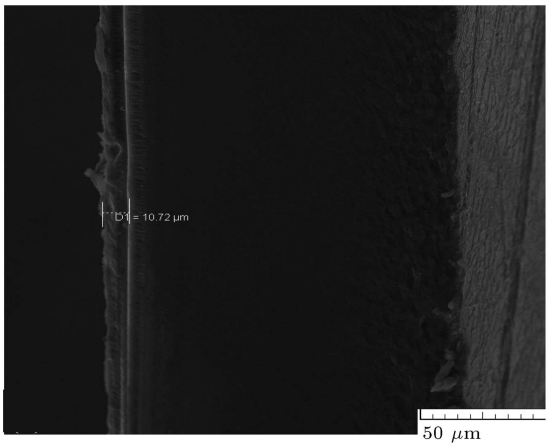

(a)

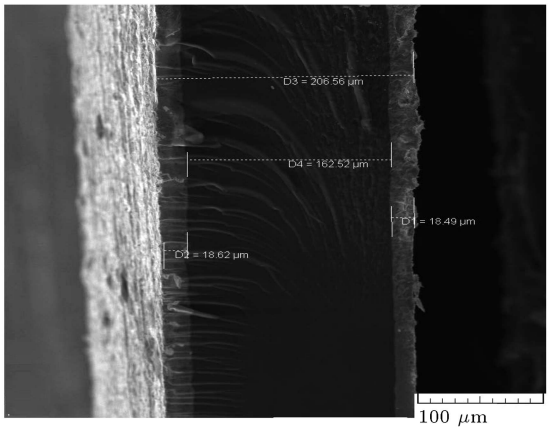

(b)

Figure 1. SEM micrographs of cross-section recycled Flemion®-based IPMC actuators after being (a) twice plated, and (b) five times plated.

be in direct correlation with the gradual distribution of solubility of water inside Flemion® membrane. Although primary plating of metallic electrode covers the whole membrane surface, high resistance of the thin metallic electrode prevents the monotonous distribution of electric current on the surface. Also, observation showed that the stiffness of the recycled membrane film was gradually increasing during the impregnation-reduction process. It was noticed that the thin metallic layer needed low force in order to be deformed compared to the thick metallic layer. This force is caused by water migration inside the film. Thereupon, it is important to have a film of optimum thickness, which results in the best deformability of an IPMC. Similar results were reported earlier for new N-IPMC [17].

The distribution of platinum particles within the cross-section of the RF-IPMC obtained by line SEM-EDX is indicated in Figure 2(a) to (c), in red color. Figure 2(a) and (b) represent the intensity after double and five-time plating, respectively. As seen, the intensity at both sides, as electrode surfaces, is the greatest while it diminishes in the bulk showing an even distribution of Pt particles within the bulk. Also, enhancement of the Pt intensity, at both sides of Figure 2(b) compared with Figure 2(a), obviously confirms the effectiveness of the plating process. The corresponding SEM-EDX map after six-time plating is also depicted in Figure 2(c), which clearly shows the smooth distribution of platinum particles on the surface and in the bulk of the RF-IPMC [18].

The top layer surface morphology of the RF-IPMC, which is mainly concerned with the electrode layer, is characterized by SEM as shown in Figure 3. Figure 3(a) and (c), and Figure 3(b) and (d) illustrate the RF-IPMC sample before and after 5 minutes of voltage application in two different magnifications, respectively. It is noteworthy that the surface of metallic part in IPMC usually appears to have micro fractures on it, which forms a particular facial topology called discrete islands [13]. As is evident from these photographs, the metallic surface over the layer appeared to be fractured, displaying discrete islands of platinum deposition. This is attributed to the tensile strength (which is less than the bending stress due to actuation of RF-IPMC) and water swelling of the polymeric membrane, which exerts an extra stress on the metallic electrodes. A similar cracked-mud structure for a new N-IPMC was also reported by Lee et al. who proposed water swelling and electroactive bending responsible for generation of these islands [17]. Furthermore, it is clear from photographs of Figure 3 that the fractured surface, as a result of voltage exerting process, increases while the size of islands decreases and is followed by the increase of water leakage from the fracture regions. Consequently, this is found to decrease the performance of RF-IPMC. Two important mechanisms of the water content reduction are water electrolysis and water vaporization. Also, water leakage outward the RF-IPMC via fractures (which are formed due to bending) could also be considered another parameter intensifying the reduction of water content during voltage application process [9].

3.2. Electrical properties

Using chronoamperometry technique, by applying a square type voltage, a typical current-time diagram was obtained for the RF-IPMC as shown in Figure 4. A step voltage of 500 mV for 3-second time intervals was applied (Figure 4(a)) and the response was obtained and exhibited in Figure 4(b). As seen, by approaching a maximum, current response shows an immediate increase by sudden variation of the voltage. Thereafter, in constant voltage, the corresponding current declines with time, exponentially, until the polarity of the electrodes is reversed, which causes an inverse current flow through the RF-IPMC. This is similar to the characteristics of an electrical capacitor as during charging, electrical charges lie on the electrodes of a capacitor. Stabilization of voltage causes fewer rooms available for charges to accumulate on the electrodes due to the capacity limitation, which consequently reduces

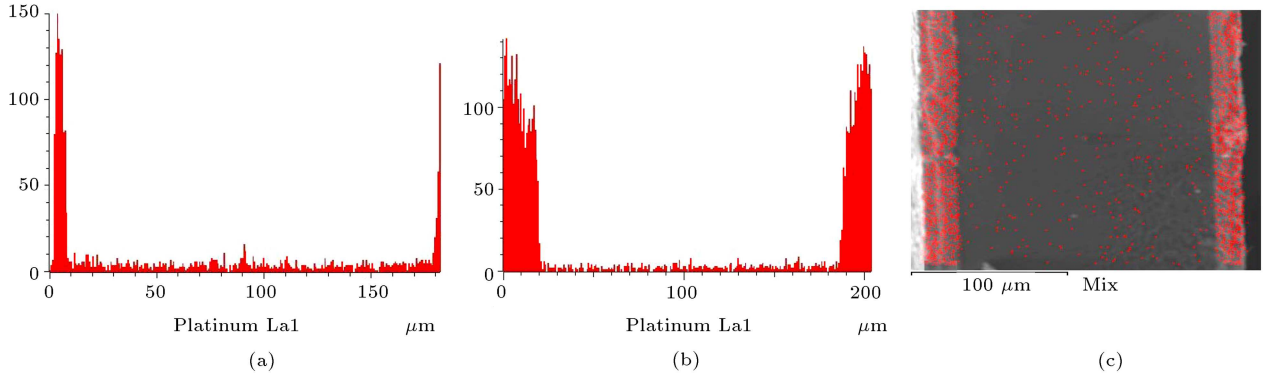

Figure 2. Line SEM-EDX analysis of Pt from the cross-section: (a) Twice plated; (b) five times plated; and (c) SEM-EDX map of Pt of the RF-IPMC.

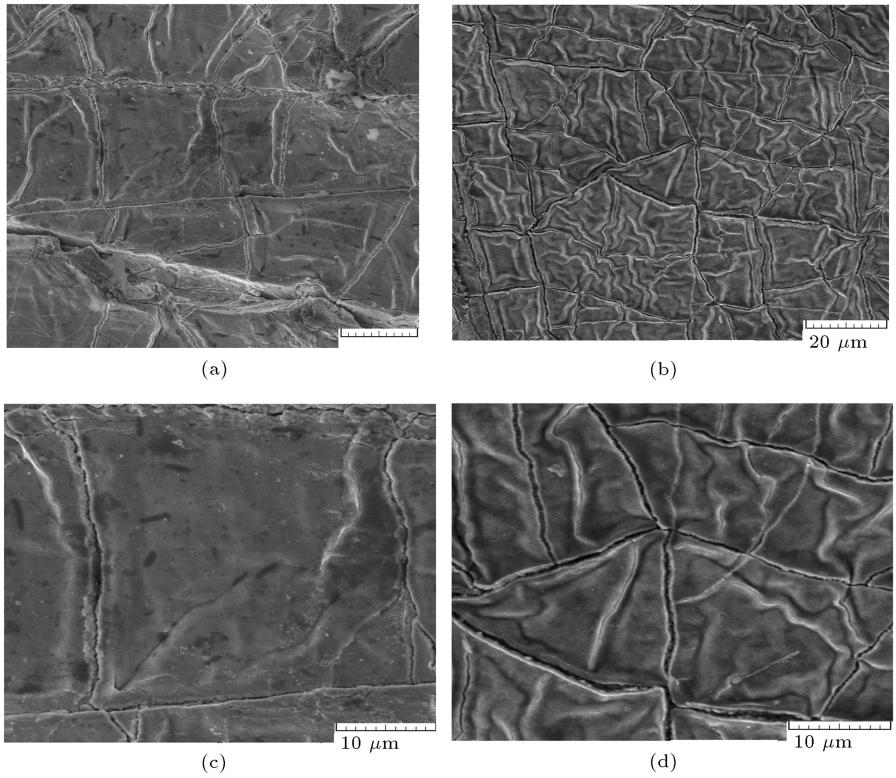

Figure 3. SEM photographs for the top layer of RF-IPMC before ((a) and (c)) and after few cycles actuation ((b) and (d)) at 2.5 V DC, magnification: (a) and (b) at 2000×, and (c) and (d) at 5000×.

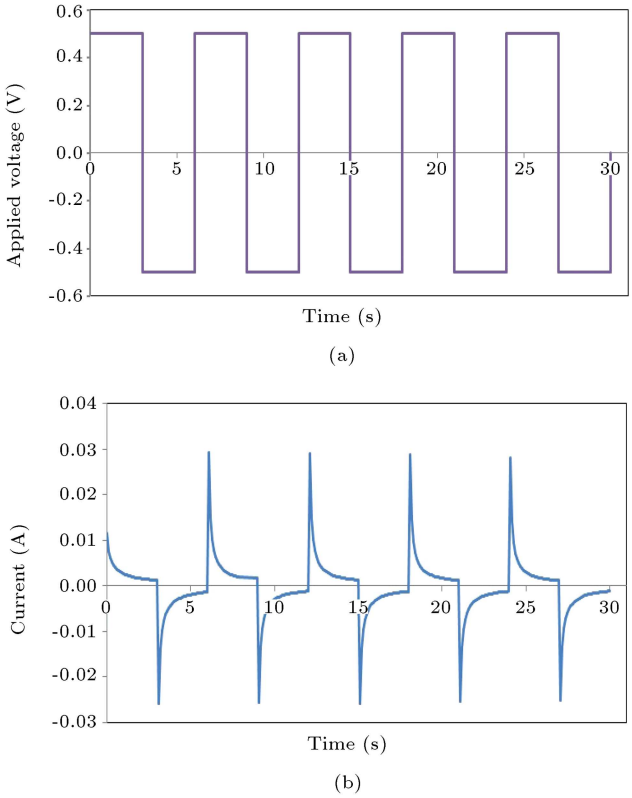

Figure 4. (a) Square-type DC voltage applied (0.5 V DC) at 3-second time intervals vs. time. (b) A typical current response vs. time for the RF-IPMC.

the electric current. Similarly, at the time of voltage application to the RF-IPMC, electrostatic forces move the cations from cathode to anode, instantaneously. Then, by keeping the voltage constant for a period of time, the rate of cation migration toward the anode decreases due to the accumulation of cations in vicinity of the cathode. In this state, the value of current passing through the RF-IPMC is a descending function of time. As a result, water molecules also move toward the anode along with cations while forming clusters with cations. This forces the RF-IPMC sample to bend. A similar behavior for a new N-IPMC was also reported by other researcher [19,20].

Figure 5(a) and (b) represent the results for the square-type low DC voltages applied within 20 to 500 mV, and the corresponding current responses as functions of time, respectively, at a constant frequency (0.16 Hz) for the RF-IPMC. The conventional current-time response explained earlier in Figure 4(b), which is also highly reproducible, can be seen, once again, even at all low voltages applied despite no observable motion of the recycled actuator. According to Figure 5(b), by increasing voltage, the peak current, I_P (mA), also increases. No offset current indicating presence of the Faradic current due to water electrolysis is observed. The response current seems to be purely due to movement of the ions through the RF-IPMC.

Figure 6(a) represents the results for the square-

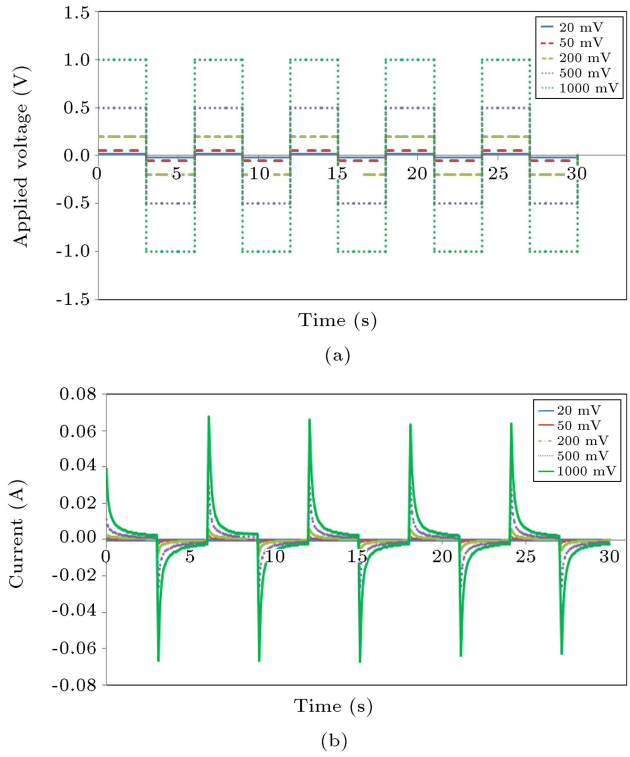

Figure 5. (a) Square-type low DC voltages vs. time. (b) Current responses vs. time for the RF-IPMC.

type high DC voltages applied within 1.0 V to 2.5 V while Figure 6(b) shows the corresponding current response vs. time at a constant frequency 0.16 Hz for the RF-IPMC. Once again, the typical current-time response, which is reproducible, can be observed within the voltage range 1 to 2.5 V; however, the sensible movement of the RF-IPMC is now observed after 1.5 V with a significant increase in the current. According to Figure 6(b), by increasing voltage, the (peak) current is also enhanced. Nevertheless an offset current is appeared mainly due to presence of the Faradic current and it develops with voltage after 1.5 V. The response (peak) current here seems to be affected both by non-Faradic current (I_{NF}) due to migration of the ions through the actuator and consequent charging of the double layers on the electrode surfaces. The Faradic current (I_F) caused by water electrolysis according to Eq. (1) is:

$$I_p = I_{NF} + I_F. \quad (1)$$

If so, then the percentage of water electrolysis or, in other words, current deficiency can be defined as:

$$\% \text{ Electrolysis} = (I_F/I_P) \times 100. \quad (2)$$

The consumed electrical charges (Q) can be estimated according to Eq. (3):

$$Q = \int I_P.dt. \quad (3)$$

To clarify this, the non-Faradic and Faradic currents

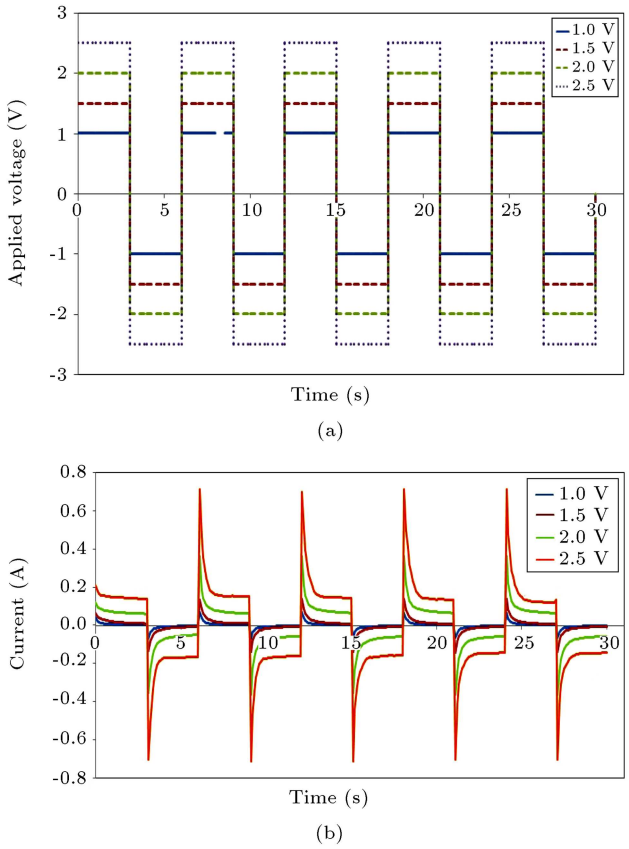

Figure 6. The effect of voltage on (a) 2 V square wave, and (b) impressive current responses vs. time for the RF-IPMC.

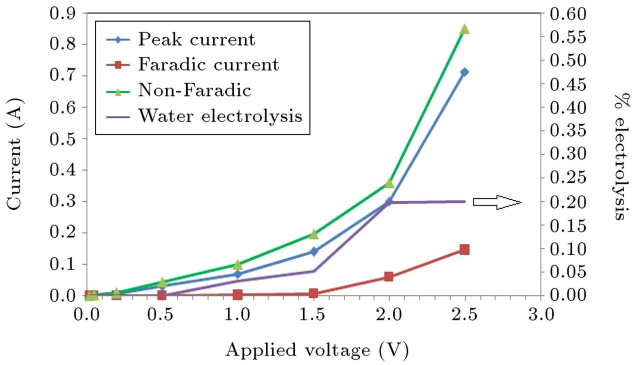

Figure 7. Graphs of peak, Faradic and non-Faradic currents along with the water electrolysis percentage as a function of applied voltage for the RF-IPMC.

(offset current), percentage of electrolysis, and the consumed electrical charges are estimated by the peak currents at various voltages from Figure 6(b) and the results are summarized in Table 1 and represented as a function of voltage in Figure 7. As seen, at low potential, there is no sign of offset or Faradic current, which is reasonable. However, over 1.5 V, which is beyond the water electrolysis potential, Faradic current and the percentage of water electrolysis appear and increase with voltage.

Table 1. Peak, Faradic and non-Faradic currents, and the percentage of water electrolysis along with the consumed electrical charges at different applied voltages for the recycled RF-IPMC.

Voltage (V)	Peak current I_P (mA)	Offset (Faradic current, I_F (mA)	Non-Faradic current, I_{NF} (mA)	% water electrolysis	Consumed electrical charges Q (mC)
0.02	1.0	0.0	1.0	0.0	0. 659
0.05	2.0	0.0	2.0	0.0	10.07
0.20	6.0	0.0	6.0	0.0	34.9
0.50	30.0	0.0	30.0	0.0	131.8
1	70.0	2.30	67.7	3.2	287.1
1.5	140.0	7.51	132.0	5.3	651.3
2	300.0	59.2	240.0	19.7	2632.6
2.5	713.0	145.8	567.0	19.9	5681.8

Shi et al. [21] also realized from an electromechanical model analysis that since they did not consider the effect of water electrolysis, the simulated result was higher than the experimental data, especially under a high voltage. Then, they arrived at the conclusion that it is essential to choose a more exact model to analyze the performance of an IPMC in the future which considers the water electrolysis and free diffusion under high voltage application.

3.3. Effect of frequency on current-time response

In order to study the effect of frequency (and therefore the resulting time period ($f = 1/T$)) input square wave voltages on the electrical behavior of the RF-IPMC, the electrical current was measured under 2.0 V applied voltage as a function of time at different frequencies. Figure 8(a) and (b) represent the current responses at two different frequencies of 0.1 and 1.0 Hz, respectively. As seen, two distinguished effects can be observed from these graphs. First, the peak current at 0.1 Hz is higher than that of 1.0 Hz. This impact is better realized with reference to Figure 9 where the results for the peak current as a function of frequency are illustrated. According to these results, peak current somewhat decreases with frequency, linearly. This is mainly because at high frequency, the capacitive characteristics of the RF-IPMC would not have sufficient time to either fully charge or discharge with the resultant current through the RF-IPMC; thus, I_p starts with a value less than its maximum achievable one. Similar results for the effect of frequency on the reduction of current density of an N-IPMC actuator within the frequency range 2 to 16 Hz were previously reported by Lee et al. [17].

Second, at high frequencies wherein the time period of the input voltage was reduced, the current was reversed before it reached its steady-state value (or current plateau). We, here, define the steady-state current value either as Faradic or zero current

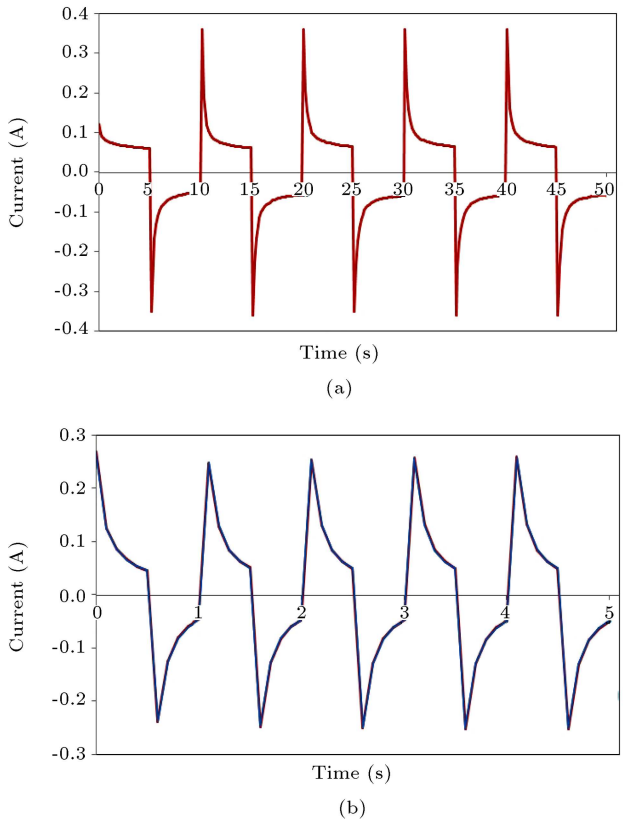

Figure 8. Current response of the RF-IPMC at 2 V and different frequencies at (a) 0.1 Hz, and (b) 1 Hz.

on the occasion or absence of water electrolysis, respectively. This, once again, has something to do with the capacitive characteristics of the IPMC or, in other word, its RC circuit behavior. According to different RC circuit models proposed for prediction of the electrical performance of an IPMC [22], an IPMC has an equivalent $R_{eq}C$ where R_{eq} is the value of the equivalent resistance of all resistance components of the IPMC in ohms, and C is the value of the capacity in Farads which is equal to time constant (τ) of the

Table 2. The current-time data at different frequencies at 2.0 V for the RF-IPMC.

Frequency (Hz)	Applied voltage period before polarity change(s) T_P	Time constant τ (s)	Transient time, at 5τ (s)	Plateau current at 5τ (mA)
0.1	**5.0**	0.56	**2.8**	0.067
0.5	**1.0**	0.34	**1.7**	Not observed
1.0	**0.5**	0.20	**1.0**	No
2.0	**0.25**	0.12	**0.6**	No

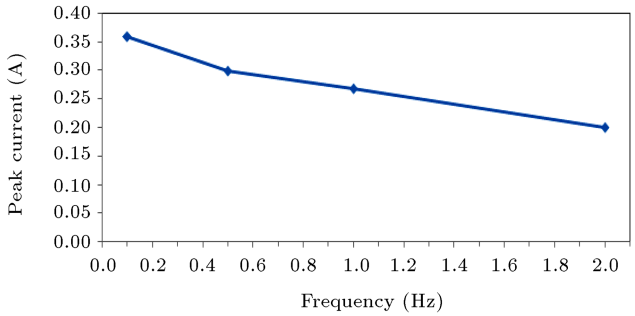

Figure 9. Peak currents of RF-IPMC as a function of frequency.

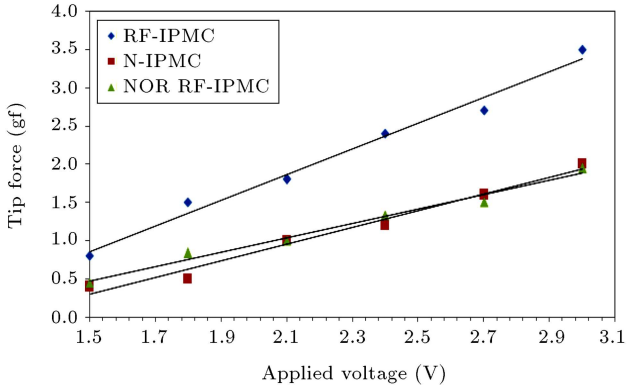

Figure 10. Maximum tip force generated by RF-IPMC and Nafion®-based IPMC actuators against applied DC voltages.

capacitor ($\tau = R_{\text{eq}} \times C$) in seconds. It is defined as the time taken by the capacitor to charge or discharge to 63% of its maximum value [22]. In such an RC circuit, the IPMC capacitor charges up gradually through its internal resistor(s) until the voltage across the IPMC capacitor reaches that of the supply voltage. The transient response time required for this to occur is equivalent to about 5 × time constant or 5τ. This transient response time, 5τ, is measured in terms of seconds.

Table 2 contains the values obtained for frequency, applied voltage period before polarity change, T_p ($T_p = T/2$), time constant τ, transient time at 5τ, and the corresponding plateau current at the input 2 V voltage applied to the recycled RF-IPMC. According to these data and by comparison of T_p with 5τ, it can be seen that only at low frequency (0.1 Hz), where T_p is greater than 5τ, the plateau current can be observed or, in other words, the capacitor is fully charged or discharged on each cycle. The prolonged voltage application ($T_p >> l5\tau$) does not have any effect on the capacitive characteristic of the recycled IPMC, except extending the time period. If T_p is less than 5τ, the RF-IPMC capacitor would not have sufficient time to either fully charge or discharge with the resulting loss of the current plateau. Of course, one expects, at T_p equal to 5τ, a perfectly matched RC waveform to be observed.

3.4. Effect of voltage on maximum tip force

The maximum tip force generated by the RF-IPMC actuator at different voltages is shown in Figure 10. For comparison purposes, that of the N-IPMC is also measured and illustrated in this figure. As the applying voltage increases, the generative tip force increases linearly for both samples; however, a high tip force was generated by the RF-IPMC compared with N-IPMC. Since the tip force depends somewhat on the thickness of the IPMC, according to previous studies [19], and as the thicknesses of the samples were slightly different (270 μm against 150 μm), the measured tip forces were normalized by dividing by their thicknesses; the results are shown in Figure 10. As seen, this time, very close results were obtained for both actuators at the same potential showing that the membrane recycling did not have a sensible effect on the mechanical performance of the RF-IPMC.

3.5. Mechanical properties

On the other hand, it has been reported that the fabrication conditions of IPMCs may influence their mechanical properties, such as tensile strength and modulus [23,24]. The bending stiffness of the IPMC samples was thus evaluated. The bending stiffness of the thin films can be measured by their Young's modulus. The flexural rigidity of a beam is represented by $E \times I$ according to the theory of solid mechanics, where E is the Young's modulus and I is the moment of inertia and the bending stiffness (B) for cantilever beam can be calculated using the formula, $B = EI/b$, where b is the width of the beam [24]. Table 3 compares

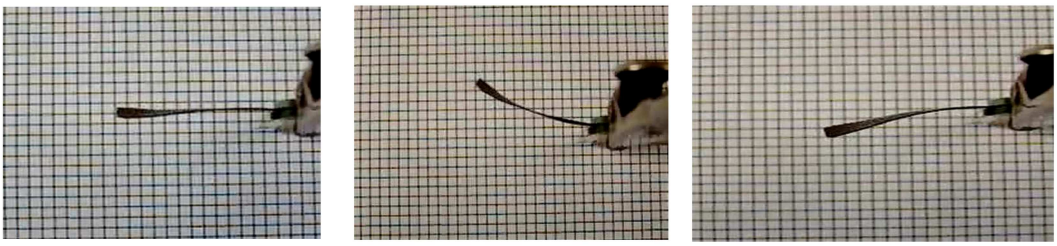

(a) (b) (c)

Figure 11. Bending of the RF-IPMC at different DC voltages: (a) At rest (0.0 V); (b) 2.0 V; and (c) -2.0 V.

Table 3. The values of Young's modulus for different IPMC samples.

Type of IPMC	Thickness (mm)	Young's modulus (MPa)	Water uptake membrane %
RF-IPMC	0.270	79	12.6
N-IPMC	0.150	72	14.1

the values of Young's modulus for RF-IPMC and N-IPMC measured in wet condition. The RF-IPMC has slightly higher Young's modulus than the N-IPMC, which may be attributed to its slightly higher thickness and/or water uptake of the Nafion® membrane as compared in Table 3. A close value (74.0 MPa) has already been reported for the Young's modulus of a Nafion®-based IPMC by other workers. Once again, no significant changes in the mechanical properties of the IPMCs were observed due to the membrane recycling.

3.6. Effect of voltage and frequency on tip displacement

A typical bending motion of the RF-IPMC actuator at rest and different DC voltages is demonstrated in Figure 11. Such IPMC bending motions were reproducible and durable for several times until all the water molecules were depleted from the IPMC's surfaces. The displacement of RF-IPMC is composed of two directional components, i.e. upward and downward components, which are somewhat different. The bending speed and displacement depend on various factors such as applied voltage and frequency, water content, surface resistance, and electrode thickness [19]. In this work, however, only the effects of voltage and frequency on tip displacement of the RF-IPMC are investigated. The maximum bending displacement is measured at the free end of the sample after sufficient elapsing time so that no more bending is observed. Figure 12(a) represents the square-type DC voltage and Figure 12(b) illustrates the corresponding tip displacement as a function of time at different applied voltages for the recycled RF-IPMC. As can be seen, the results exhibit a good

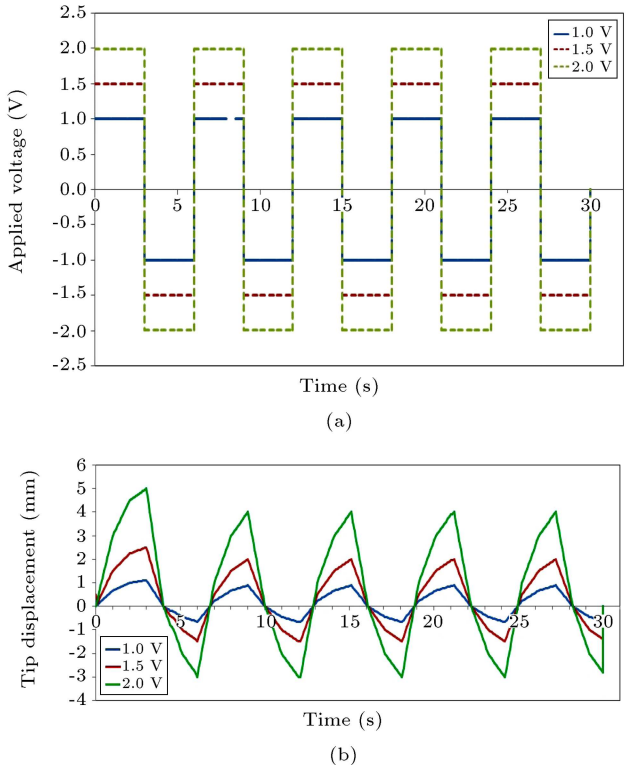

Figure 12. (a) Applied square-type DC voltage (1-2 V) as a function of time. (b) Corresponding tip displacement for the RF-IPMC.

relationship between the maximum displacement and the applied voltage at different times. Also, the results demonstrate that displacement increases with increase in the potential, as clearly shown for downward and upward maximum displacement graphs in Figure 13. A higher displacement at upward in respect of downward movement at the same input voltage cannot be due to the weight of RF-IPMC as in that case, it should exhibit less displacement while going upward. Hunt et al. [25] explained this phenomenon as the IPMC's shape hysteresis which is caused by delayed solvent migration and redistribution compared with rapidly transferred ions within the membrane. On the effect of frequency on the tip displacement, our observations revealed that the type of movement of the RF-IPMC changes from bending motion at low frequencies (T_P longer than 5τ) to vibration mo-

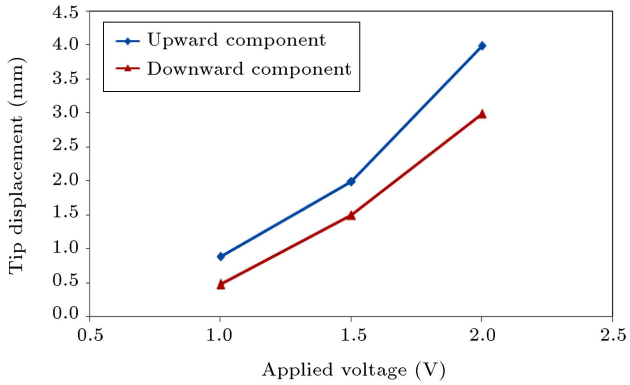

Figure 13. Maximum tip displacement at downward and upward bending at different DC voltages for the RF-IPMC.

tion at higher frequencies (T_p equal to or less than 5τ). Depending on the type of application desired for an IPMC, different frequencies can be applied to control the type and the rate of movements of an IPMC.

4. Conclusions

The perfluorinated Flemion® membrane recycled from a used composite chlor-alkali membrane was coated by platinum electroless plating to form a low-cost IPMC. Morphology, particle distribution, electrical and mechanical performances of the recycled IPMC were studied and compared with those of a new Nafion®-based IPMC. According to morphology studies, an even distribution of platinum particles on the surface and in the bulk of the recycled IPMC was clearly demonstrated by line SEM-EDX. A conventional fractured metallic surface layer displaying discrete islands was formed, in which the number of islands increased while their size decreased by voltage application. A typical current-time diagram, which was highly reproducible, was also obtained for the recycled IPMC at low voltages with a significant increase in the current and appearance of an offset current developing with voltage over 1.5 V. A basis was introduced so that only at low frequencies corresponding to $T_p \geq 5\tau$, the plateau current caused by full charging or discharging of the RF-IPMC, could be observed. The peak current also decreases with frequency, linearly. Very close values for Young's modulus and normalized maximum tip force generated by both IPMCs were obtained confirming that the recycling did not have a sensible effect on the mechanical performance of the recycled IPMC. A typical bending motion, which was reproducible and durable, was shown by the RF-IPMC. Finally, the used membranes from chlor-alkali and/or water electrolysis industries were found to be rich resources for manufacturing low cost IPMCs.

References

1. Shahinpoor, M., Kim, K. and Mojarrad, M., *Artificial Muscles Applicants of Advanced Polymeric Nanocomposites*, Taylor & Francis, New York (2007).
2. Kim, K.J. and Tadokoro, S.O., *Electroactive Polymer for Robotic Application*, Springer-Verlag, London (2007).
3. Shahinpoor, M. and Kim, K. "Ionic polymer-metal composites: I. Fundamentals", *J. Smart Mater. Struct.*, **10**, pp. 819-833 (2001).
4. Wang, J., Xu, C., Taya, M. and Kuga, Y. "A Flemion®-based actuator with ionic liquid as solvent", *J. Smart Mater. Struct.*, **16**, pp. S214-S219 (2007)
5. Kim, K.J. and Shahinpoor, M. "Ionic polymer-metal composites: II. Manufacturing techniques", *J. Smart Mater. Struct.*, **12**, pp. 65-79 (2003).
6. Shahinpoor, M. and Kim, K. "Novel ionic polymer-metal composites equipped physically loaded particulate electrodes as biomimetic sensors", *J. Sens. Actuators A.*, **96**, pp. 125-132 (2002).
7. Fang, B.K., Ju, M.S. and Lin, C.K. "A new approach to develop ionic polymer-metal composites (IPMC) actuator: Fabrication and control for active catheter systems", *J. Sens. Actuators A.*, **137**, pp. 321-329 (2007).
8. Wang, X.L., Oh, I.K., Lu, J., Ju, J.H. and Lee, S. "Biomimetic electro-active polymer based on sulfonated poly (styrene-b-ethylene-co- butylene-b-styrene)", *J. Mater. Letters*, **61**, pp. 5117-5120 (2007).
9. Luqman, M.H., Lee, J.W., Moon, K.K. and Yoo, Y.T. "Sulfonated polystyrene-based ionic polymer-metal composite (IPMC) actuator", *J. Indust. Eng. Chem.*, **17**, pp. 49-55 (2011).
10. Newbury, K.M. and Leo, D.J. "Linear electromechanical model of ionic polymer transducers - Part I: Model development", *Journal of Intelligent Material Systems and Structures*, **14**, pp. 333-342 (2003).
11. Jung, K., Nam, J. and Choi, H. "Investigations on actuation characteristics of IPMC artificial muscle actuator", *Sensors and Actuators A (Physical)*, **107**, pp. 183-92 (2003).
12. Nemat-Nasser, S. and Zamani, S. "Modeling of electrochemomechanical response of ionic polymer-metal composites with various solvents", *Journal of Applied Physics*, **100**, p. 064310 (2006).
13. Jung, W. and Toi, Y. "Finite element analysis of ionic-conducting polymer metal composite actuators using Flemion®", *Proc. IMECS*, **II**, Hong Kong (2009).
14. Mohammadi, F. "Recyclimg and recasting of used chlor-alkali membranes", Project contract No. 0890138701, NPC- RT Co, Tehran, Iran (2010).
15. Mohammadi, F. and Rabiee, A. "Solution casting, characterization, and performance evaluation of perfluorosulfonic sodium type membranes for chlor-alkali application", *J. Appl. Poly. Sci.*, **120**, pp. 3469-3476 (2011).

16. Siroma, Z., Fujiwara, N., Ioroi, T., Yamazaki, S., Yasuda, K. and Miyazaki, Y. "Dissolution of Nafion® membrane and recast Nafion® film in mixtures of methanol and water", *J. Power Sources.*, **126**, pp. 41-45 (2004).

17. Lee, J.H., Lee, J. Hoon., Nam, J.D. and Choi, H.K. "Water uptake and migration effects of electroactive ion-exchangepolymer metal composite (IPMC) actuator", *J. Sens. Actuators A.*, **118**, pp. 98-106 (2005).

18. Jei, C., Chen, T.S., Hsieh, L.C. and Fa, M. "Preparation of gradually componential metal electrode on solution-casted Nafion® membrane", *J. Bio. Eng.*, **24**, pp. 434-437 (2007).

19. Kim, S.M. and Kim, K.J. "Ionic polymer-metal composites (IPMCs) with bimetallic Pt-Pd electrode", *Proc. SPIE*, **6927**, 69270D/1-69270D/7 (2008).

20. Asaka, K., Oguro, K., Nishimura, Y., Mizuhata, M. and Takenaka, H.Y. "Bending of polyelectrolyte membrane-platinum composites by electric stimuli I. Response characteristics to various waveforms", *J. Polymer.*, **4**, pp. 436-440 (1995).

21. Shi, L., Juo, S.X. and Asaka, K. "Modeling and experiments of IPMC actuators for the position precision of underwater legged microrobots", *Proceeding of the 2012 IEEE*, pp. 420-425 (2012).

22. Electronics Tutorial about the RC Time Constant, http://www.electronics-tutorials.ws/rc/rc_1.html.

23. He, Q.S., Yu, M., Song, L., Ding, H., Zhang, X.Q. and Dai, Z.D. "Experimental study and model analysis of the performance of IPMC membranes with various thickness", *J. Bionic. Eng.*, **8**, pp. 77-85 (2011).

24. Panwar, V., Cha, K.G., Park, J.O. and Park, S. "High actuation response of PVDF/PVP/PSSA based ionic polymer metal", *J. Sens. Actuators B: Chem.*, **161**, pp. 460-470 (2012).

25. Hunt, A., Chen, Z., Tan, X. and Kruusmaa, M. "Control of an inverted pendulum using an ionic polymer-metal composite actuator", *Advanced Intelligent Mechatronics (AIM), IEEE/ASME*, pp. 163-168 (2010).

Biographies

Saeed Taghavi is an MSc student of Polymer Engineering at Iran Polymer and Petrochemical Institute (IPPI), Tehran, Iran. He received a BSc degree in Polymer Engineering from Darab Branch, Islamic Azad University, Darab, Iran, in 2010. His main areas of interest are nanocomposite, electroactive polymer, and biopolymer.

Fereidoon Mohammadi is Assistant Professor of Chemical Engineering in Petrochemicals Synthesis Department, IPPI, Tehran, Iran. He received a BSc degree in Petrochemical Engineering from Amirkabir University of Technology, Tehran, Iran, in 1988, and MSc and PhD degrees in Chemical Engineering from University of New South Wales Sydney, Australia, in 1993 and 1997, respectively. His main area of interest includes ion exchange membrane fabrication and recycling and electromembrane processes, such as PEM fuel cell, chlor-alkali, and ionic polymer-metal composite.

Jalal Barzin is Associate Professor of Polymer Engineering in Biomaterials Department, IPPI, Tehran, Iran. He received a BSc degree in Chemical Engineering from Isfahan University of Technology, Isfahan, Iran; and MSc and PhD degrees in polymer engineering from IPPI, Tehran, Iran, in 1997 and 2003, respectively. His main research interests are membranes in biomaterials and tissue engineering, thermodynamic of polymer solutions, and phase inversion studies and membranes cleaning.